AD_____

Award Number: DAMD17-97-1-7190

TITLE: The Design and Emulation of a Multiple-Camera SPECT Breast Imager

PRINCIPAL INVESTIGATOR: John Sain
Dr. H. Barrett

CONTRACTING ORGANIZATION: University of Arizona
Tucson, Arizona 85722-3308

REPORT DATE: July 2000

TYPE OF REPORT: Final

PREPARED FOR: U.S. Army Medical Research and Materiel Command
Fort Detrick, Maryland 21702-5012

# REPORT DOCUMENTATION PAGE

OMB No. 074-0188



| 1. AGENCY USE ONLY (Leave blank) | 2. REPORT DATE | 3. REPORT TYPE AND DATES COVERED |
|---|---|---|
| | July 2000 | Final (19 May 97 - 30 Jun 00) |

**4. TITLE AND SUBTITLE**
The Design and Emulation of a Multiple-Camera SPECT Breast Imager

**5. FUNDING NUMBERS**
DAMD17-97-1-7190

**6. AUTHOR(S)**
John Sain Dr. H. Barrett

**7. PERFORMING ORGANIZATION NAME(S) AND ADDRESS(ES)**
University of Arizona
Tucson, Arizona 85722-3308

**E-MAIL:**
cardhous@gonzo.radiology.arizona.edu

**8. PERFORMING ORGANIZATION REPORT NUMBER**

**9. SPONSORING / MONITORING AGENCY NAME(S) AND ADDRESS(ES)**
U.S. Army Medical Research and Materiel Command
Fort Detrick, Maryland 21702-5012

**10. SPONSORING / MONITORING AGENCY REPORT NUMBER**

**11. SUPPLEMENTARY NOTES**

**12a. DISTRIBUTION / AVAILABILITY STATEMENT**
Approved for public release; distribution unlimited

**12b. DISTRIBUTION CODE**

**13. ABSTRACT** ***(Maximum 200 Words)***

The **purpose** of this study has been to design and emulate a multiple-camera dedicated SPECT breast imager. The **scope** of this study involved characterizing radioactivity within a human breast, building breast phantoms for imaging, modeling mean detector responses, optimizing the system geometry, collecting planar projection data, measuring detector performance for the task of detecting signals in random backgrounds, emulating the system point response function, and generating three-dimensional reconstructions of the radioactivity distribution within the breast phantoms. **Major results** have included estimated percentage of total injected activity taken up by one breast of average mass (0.08%), estimated activity per unit mass of normal breast tissue (43 decays/second), and estimated maximum relative uptake ratio (6:1). Human breast and torso phantoms were constructed. Camera responses were measured and accurately modeled, and the camera model was used to help design a prototype camera. Planar projection data of a breast phantom was collected, and the performance of a camera for the task of detecting lesions as a function of diameter and depth was measured, indicating that 10-mm diameter lesions were reliably detected at depths up to 6 cm. A **significant problem** was the failure of an essential computer system in Year 2.

**14. SUBJECT TERMS**
Breast Cancer, mammoscintigraphy, SPECT, gamma camera, Technetium-99m

**15. NUMBER OF PAGES**
41

**16. PRICE CODE**

| 17. SECURITY CLASSIFICATION OF REPORT | 18. SECURITY CLASSIFICATION OF THIS PAGE | 19. SECURITY CLASSIFICATION OF ABSTRACT | 20. LIMITATION OF ABSTRACT |
|---|---|---|---|
| Unclassified | Unclassified | Unclassified | Unlimited |

NSN 7540-01-280-5500

Standard Form 298 (Rev. 2-89)
Prescribed by ANSI Std. Z39-18
298-102

## FOREWORD

Opinions, interpretations, conclusions and recommendations are those of the author and are not necessarily endorsed by the U.S. Army.

___ Where copyrighted material is quoted, permission has been obtained to use such material.

___ Where material from documents designated for limited distribution is quoted, permission has been obtained to use the material.

___ Citations of commercial organizations and trade names in this report do not constitute an official Department of Army endorsement or approval of the products or services of these organizations.

N/A In conducting research using animals, the investigator(s) adhered to the "Guide for the Care and Use of Laboratory Animals," prepared by the Committee on Care and use of Laboratory Animals of the Institute of Laboratory Resources, national Research Council (NIH Publication No. 86-23, Revised 1985).

N/A For the protection of human subjects, the investigator(s) adhered to policies of applicable Federal Law 45 CFR 46.

N/A In conducting research utilizing recombinant DNA technology, the investigator(s) adhered to current guidelines promulgated by the National Institutes of Health.

N/A In the conduct of research utilizing recombinant DNA, the investigator(s) adhered to the NIH Guidelines for Research Involving Recombinant DNA Molecules.

N/A In the conduct of research involving hazardous organisms, the investigator(s) adhered to the CDC-NIH Guide for Biosafety in Microbiological and Biomedical Laboratories.

John D. Sain 7-25-00

PI - Signature Date

## Table of Contents

## INTRODUCTION

Proper staging and management of breast cancer depends on early and accurate diagnosis of primary and/or metastatic cancer. Single-photon emission computed tomography (SPECT), used in conjunction with x-ray mammography, might increase the probability of an accurate diagnosis. The purpose of this study has been to design and emulate a multiple-camera dedicated SPECT breast imager. Experimental procedures have included: (a) characterizing radioactivity within the human breast, (b) building breast phantoms for imaging, (c) modeling mean detector responses, (d) optimizing the system geometry, (e) collecting planar projection data for the small and large cameras, (f) measuring detector performance for the task of detecting signals in random uniform and non-uniform backgrounds, (g) emulating the system point response function, and (h) generating three-dimensional reconstructions of the radioactivity distribution within the breast phantom. This final report, while reporting in more detail on the work completed in Year 3 of the grant, provides a summary of all the work accomplished under this grant.

*Please note:* The outline for the "body" and "conclusions" sections of this report follow the revised Statement of Work submitted April 3, 2000, as requested by my Contracting Officer Representative. Please refer to Appendix A for the details.

## OBJECTIVE 1: Construction of Breast Phantoms

*Task 1. Characterize the expected radiotracer activity within the breast.*

In clinical studies a standard injection of Tc-99m Sestamibi into a patient contains 20 mCi of activity. A minute fraction of this activity ends up in the breasts. The estimated percentage of the original injected activity taken up by a single breast of average mass (410 g, according to the Cristy-Eckerman model) is about 0.08 %, which corresponds to about 16 uCi. The estimated activity per unit mass of normal breast tissue is about 43 dpm/mg. [Year 1 Annual Report, pp. 6-8.]

The uptake of Tc-99m Sestamibi by abnormal types of tissue (relative to normal breast tissue) varies. Fatty tissue tends to take up about the same amount as normal tissue. Malignant tumors, on the other hand, typically exhibit high relative uptakes. The degree of uptake appears to vary significantly with the histological type of the tumor and not the histological grade. For example, ductal and lobular carcinomas exhibit a relative uptake ratio of nearly 6:1 and fibroadenomas nearly 3:1. Other types of abnormalities, such as inflammations, fibrocystic disease, and sclerosing adenoses, have been known to occasionally take up a significant amount of Tc-99m Sestamibi, but the uptake is not consistently high. The relative uptake ratio can range from 1:1 to 3:1. Some abnormalities, such as cysts, benign tumors, and epithelial hyperplasia, typically exhibit low relative uptakes, or uptakes similar to normal breast and fatty tissue. [Year 1 Annual Report, pp. 8-12.]

*Task 2. Build a realistic model of the human breast and adjacent chest wall.*

A model of a female torso containing breast, heart, and liver phantoms has been constructed. The breast phantom comes in two sizes and is capable of holding several hot and/or cold lesions (See Fig. A). The lesions are modeled by water-filled plastic spheres of various diameters (See Fig. B) and can be located anywhere within the breast phantom. The torso model represents a human torso from the shoulders to the hips. Both heart and liver phantoms can be placed inside it (See Figs. C-D). Thus, specific levels of radioactivity in the main torso, heart, and liver may be modeled.

The complete model represents a prone female with one pendant breast. Clinical imaging studies favor the prone position (over the erect position) because it allows for better visualization of deep mammary tissue without any significant interference from activity present in the thoracic cavity. [Year 1 Annual Report, pp. 13-14.]

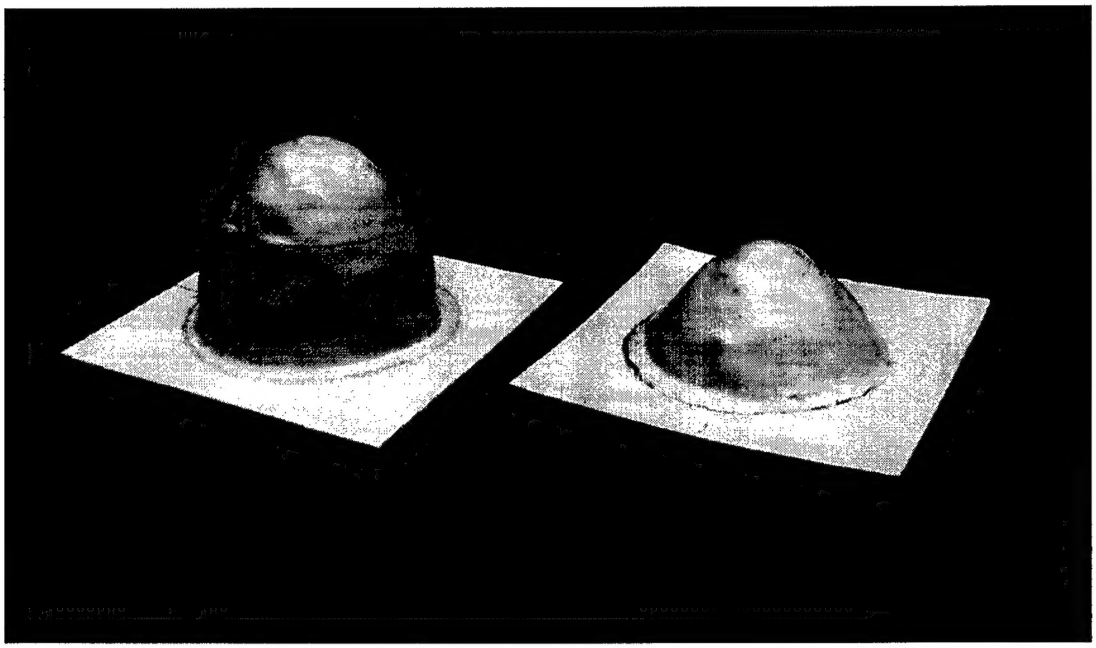

**Fig. A** Breast phantoms. Two breast phantoms were made out of NCM Clinic D thermoplastic. Each phantom represents a pendant breast with a base diameter (at the chest wall) of 10 cm. The volumes of the large and small phantoms are 540 ml and 210 ml, respectively, while the base-to-nipple dimensions are 8 cm and 5 cm, respectively.

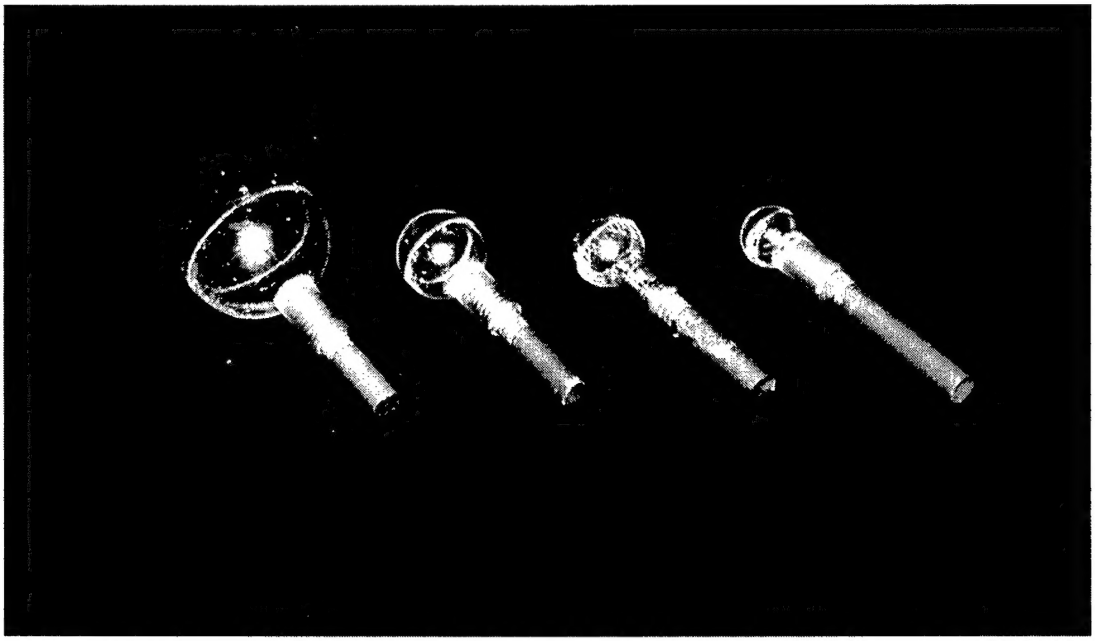

**Fig. B** Some of hollow plastic spheres used to simulate lesions. Several hollow plastic spheres, with diameters ranging from 4 to 28 mm, were procured to simulate lesions. Each sphere can be mounted to the base of the breast phantom with a thin plastic rod. A wide variety of single/multiple-lesion scenarios can be modeled.

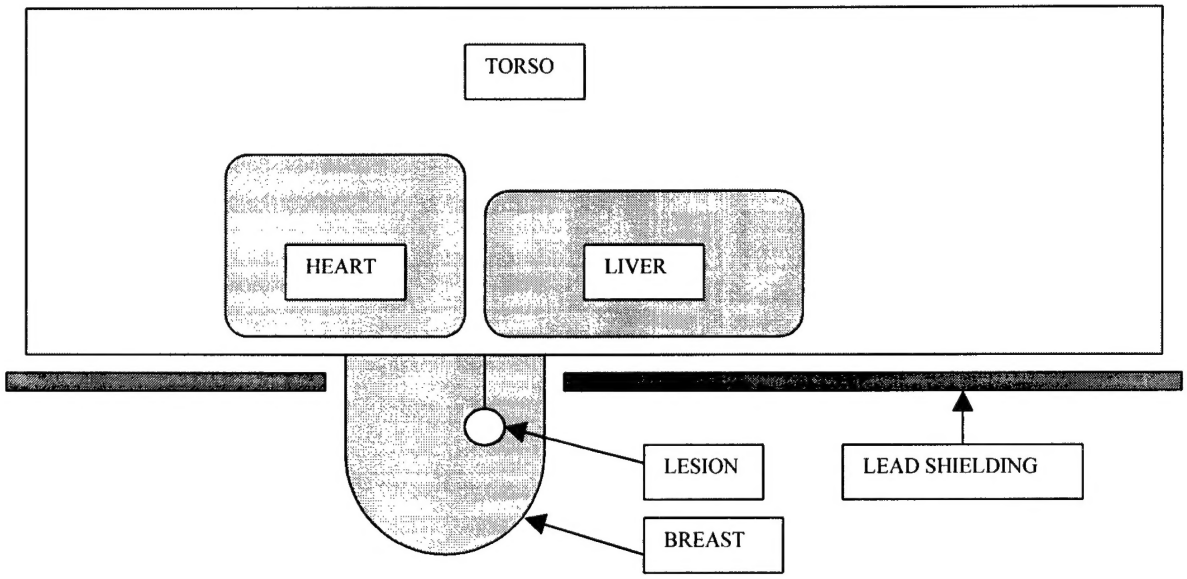


**Fig. C** Schematic of female torso phantom.

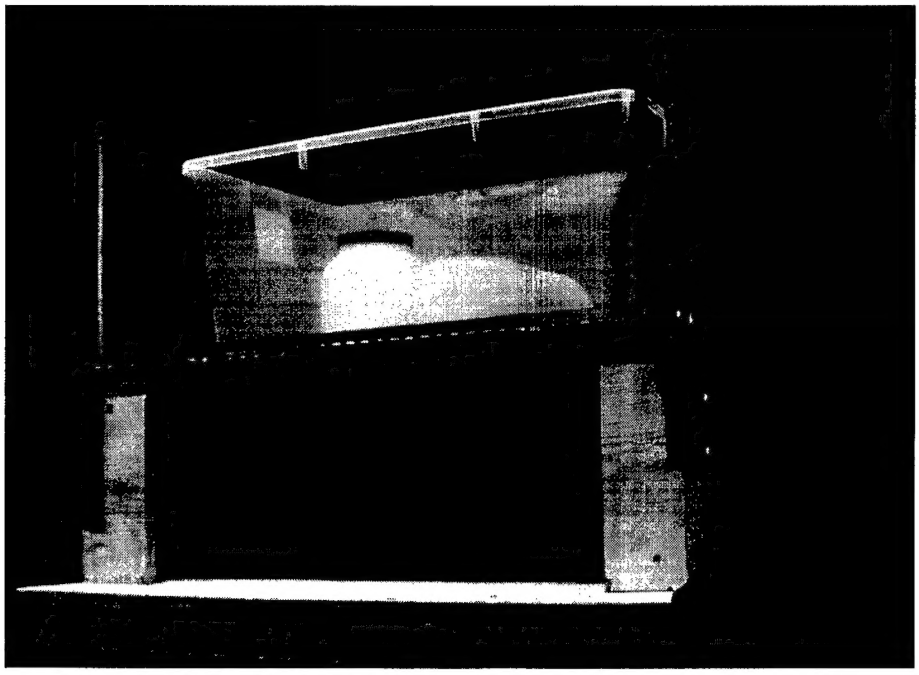

**Fig. D** Female torso phantom containing heart, liver, and breast phantoms. Prone imaging of a single breast provides maximum separation of the breast tissue from the myocardium and liver. The torso was emulated with a plastic storage container (42 cm W x 65 cm L x 30 cm H). Smaller watertight plastic storage containers, representing the heart and liver, were placed inside the torso phantom. Different levels of radioactivity in the main torso, heart, and liver may be modeled.

## OBJECTIVE 2: Design and Emulation of Imaging System

*Task 3. Characterize the response of the small modular gamma cameras.*

The mean response of the small modular gamma cameras has been characterized in the laboratory using two tools: (1) a "mean detector response function (mdrf)" and (2) a "point array". An mdrf provides an accurate measure of the mean response of the camera (in terms of its photomultiplier tube signals) to a gamma ray incident anywhere on the camera face. A common diagnostic plot is a diagonal of the mdrf contour for a single photomultiplier tube -- the diagonal that passes through the location of the center of the photomultiplier tube. A point array illustrates the spatial resolution of the camera as a function of position on the camera face. The array image is a histogram of the estimated locations where unscattered gamma rays struck the camera face. Since the image is essentially an array of points, the spatial resolution of the camera can be qualitatively analyzed. [Year 1 Annual Report, pp. 15-17.]

An optical model was developed which provides an estimate of the camera response to a gamma ray incident anywhere on the camera face. The optical model, taking into account the physical and optical properties of the camera components, performs radiometric calculations to determine the fate of all of the light emitted by a scintillation event. In particular, the amount of light detected by each photomultiplier tube is calculated, so the mean response of any photomultiplier tube to a scintillation event located anywhere within the scintillation crystal can be estimated. The data generated by the model nearly matches the data obtained from a real camera in the laboratory. [Year 1 Annual Report, pp. 17-19.]

*Task 4. Characterize the response of the large modular gamma camera.*

The estimated mean response of the large modular gamma camera has been characterized. An optical model, very similar to the model of the small camera, was developed which provides an estimate of the camera response to a gamma ray incident anywhere on the camera face. Given that the small and large cameras are so similar in design, the assumption is that the model, which worked so well for the small camera, would also work well for the large camera. [Year 1 Annual Report, pp. 20-22.]

Comparison to real camera data will be available very soon. The optical model has been used to design and recently (Spring 2000) build a prototype modular gamma camera using a 3x3 array of photomultiplier tubes (See Fig. E). Work is currently underway to measure an mdrf and point array for this prototype camera.

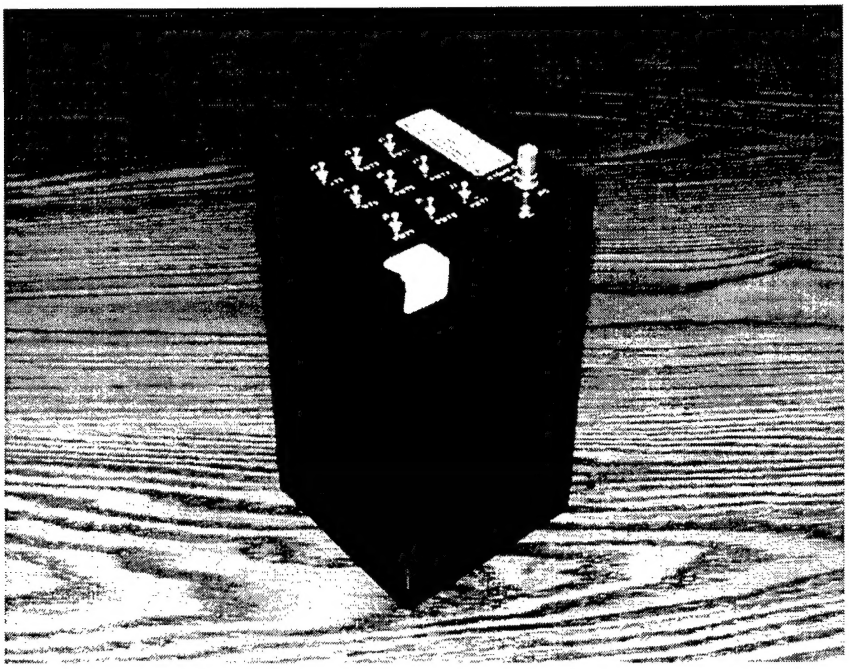

**Fig. E** Newly designed 3x3 modular gamma camera.

*Task 5. Optimize the geometry of the system configuration.*

The purpose of the optimization of the geometry of the system configuration was to define the position and field of view of each camera, the type, size, and arrangement of aperture for each camera, and the magnification of the object. As noted in the Year 1 annual report, such optimization is a process that goes hand in hand with determining how well the system can detect various types of lesions within a breast. Thus, the optimization has continued as the system capabilities have evolved.

In Year 1 of this grant, two significant modifications occurred. First, the orientation of the small cameras was slightly changed. Second, the pinhole apertures for the small cameras were replaced with parallel-hole collimators. [Year 1 Annual Report, pp. 23-24.]

In Year 2 of this grant, a general-purpose parallel-hole collimator was selected. The collimator has a 23.6-mm bore length, a 1.5-mm bore diameter, and an efficiency of 0.01%. [Year 2 Annual Report, p. 6.]

In Year 3 of this grant, initial imaging studies (as proposed in the Year 2 annual report) were done with this collimator to begin characterizing the performance of the camera with respect to collimator resolution, object-to-camera distance, and data collection times. Some of the results from these studies are described in Task 13. Conclusions made to date in these studies have not lead yet to any specific optimizations of the system geometry.

*Task 13. Evaluate performance of small modular gamma camera.*

An important aspect of the proposed imaging system is its ability to detect lesions within the breast. In particular, one would like to know the smallest lesion that the system can reliably detect and how the depth of the lesion within the tissue affects the system performance. The goal of this task was to measure the performance of the modular cameras for the task of detecting lesions as a function of diameter and depth. The results will aid in the continuing design of the imaging system.

A major portion of the collected data was summarized and recently presented in poster format at a recent conference [1]. Please refer to Appendix B of this report for a complete copy of the poster.

**Objective 3: Development of Software**

*Task 7. Emulate the system point spread function.*

The system point spread function has not been emulated. The principal investigator made the choice to fully evaluate the detectability performance of the small modular gamma camera in order to increase his understanding of the performance of the camera (See Task 13), and this effort, while quite successful, encroached upon the time allocated to set up for and measure the point spread function of the system. It may be argued that the increased understanding of how well the cameras can detect lesions will contribute to a better understanding of how the system geometry should be optimized, thus leading to a better configuration prior to measuring a point spread function.

*Task 8. Develop an algorithm to generate three-dimensional reconstructions of the injected radiotracer activity.*

An algorithm has not been developed. As noted in the proposal, robust algorithms of the required type are already extensively used within this research group. An investigation of which algorithm might be best suited for this imaging system were supposed to begin once the principal investigator had both a system point spread function and projection data from each of the cameras. A system point spread function has not been measured, and so no work has been done on algorithm selection.

**Objective 4: Collection of Data and Reconstruction of Images**

*Task 9. Collect and estimate projection data for small cameras.*

Projection data for the small cameras has been collected. Sample projection images of the large breast phantom with and without a lesion have been generated. [Year 2 Annual Report, p. 7]

*Task 10. Collect and estimate projection data for large camera.*

Projection data for the large camera has been collected and estimated. Sample projection images of the large breast phantom without a lesion have been generated. [Year 2 Annual Report, p. 8]

*Task 11. Generate three-dimensional reconstructions of the radiotracer distribution.*

Three-dimensional reconstructions of the radiotracer distribution have not been generated. A system point spread function is required, and since a system point spread function has not been measured, no reconstructions have been completed.

## KEY RESEARCH ACCOMPLISHMENTS

- Characterized the expected radiotracer activity within the human breast. Both the estimated activity per unit mass of normal breast tissue and the estimated relative uptake ratio as a function of histological type and/or grade of tumor were calculated.
- Constructed realistic phantoms of the human breast, with or without lesions, and the human torso for use in imaging studies.
- Characterized the actual mean response of the small modular gamma camera.
- Developed an optical model (in software) of the small modular gamma camera that provided estimates of the camera response to gamma rays incident anywhere on the camera face. The model output closely matched the measured laboratory response.
- Using the optical model, emulated the mean response of the large modular gamma camera.
- Collected planar images (projections) of the large breast phantom with the small camera. The phantom sometimes contained a "hot" or "cold" lesion.
- Emulated planar images (projections) of the breast phantom for the proposed large camera by combining several shifted but overlapping small camera images.
- Partially optimized the geometry of the system configuration by improving the camera positions and fields of view.
- Using the optical model, helped design a prototype large modular gamma camera, two versions of which have been recently built.
- Evaluated the performance of the small modular gamma camera for the task of detecting lesions as a function of diameter and depth.

## REPORTABLE OUTCOMES

Presentations

Sain JD and Barrett HH. "Performance evaluation of a modular gamma camera using detectability index." *The Society of Nuclear Medicine 47th Annual Meeting*, St. Louis, MO, June 4-7, 2000.

Sain JD. "The design and emulation of a multiple-camera SPECT breast imager." *Era of Hope Department of Defense Breast Cancer Research Program Meeting*, Atlanta, GA, June 8-12, 2000.

Degrees

| | | |
|---|---|---|
| Ph.D. Optical Sciences | University of Arizona | 2000 (to be awarded) |

## CONCLUSIONS

### Objective 1: Construction of Breast Phantoms

The tasks in this objective were to characterize the expected radiotracer activity within the breast (*Task 1*) and to build a realistic model of the human breast and adjacent chest wall (*Task 2*). Knowledge of how much radioactivity is typically taken up by a breast allows the system designer to ensure that the imaging system is sensitive enough to collect sufficient image data within a reasonable time frame. Realistic models of the breast and the adjacent torso allow for laboratory testing of the imaging system as the design optimization progresses.

*Task 1. Characterize the expected radiotracer activity within the breast.*

For a clinical study involving an injection of 20 mCi of Tc-99m Sestamibi, the estimated percentage of the original injected activity taken up by a single breast of average mass is about 0.08%, which corresponds to about 16 uCi. The estimated activity per unit mass of normal breast tissue is about 43 decays per minute per milligram.

The uptake of Tc-99m Sestamibi by abnormal types of tissue (relative to normal breast tissue) varies. Fatty tissue tends to take up about the same amount as normal tissue. Malignant tumors, on the other hand, typically exhibit high relative uptake ratios – of up to 6:1. The degree of uptake appears to vary significantly with the histological type of the tumor and not the histological grade.

*Task 2. Build a realistic model of the human breast and adjacent chest wall.*

A model of a prone female torso containing breast, heart, and liver phantoms has been constructed. The breast phantom comes in two sizes and is capable of holding several hot and/or cold lesions. The lesions are modeled by water-filled plastic spheres of various diameters and can be located anywhere within the breast phantom. The torso model represents a human torso from the shoulders to the hips. Both heart and liver phantoms can be placed inside it. Thus, specific levels of radioactivity in the main torso, heart, and liver may be modeled.

### Objective 2: Design and Emulation of Imaging System

The tasks in this objective were to characterize the response of the small modular gamma cameras (*Task 3*), emulate the response of the large modular gamma camera (*Task 4*), and to optimize the geometry of the system configuration (*Task 5*). Knowledge of the camera responses plays a role in determining (and improving) the sensitivity, the field of view, and the performance of the imaging system.

*Task 3. Characterize the response of the small modular gamma camera.*

The mean response of a small modular gamma camera has been characterized in the laboratory. An optical model (in software) was also developed to provide an estimate

of the mean camera response to a gamma ray incident anywhere on the camera face. The model data closely matches the laboratory data for a real camera.

*Task 4. Characterize the response of the large modular gamma camera.*

Using the optical model developed in Task 3, the estimated mean response of the large modular gamma camera has been characterized. No comparison to real data has been made yet. The optical model was recently used to help design and build a prototype large camera, but the measurements of the camera responses have not been completed.

*Task 5. Optimize the geometry of the system configuration.*

Due to concerns about out-of-field activity from the heart and liver, the most significant modifications to the geometry of the system configuration were made in an effort to eliminate as much intrathoracic activity as possible from the system field of view. The pinhole apertures for the small cameras were replaced with parallel-hole collimators, and the orientation of the small cameras was changed such that their field of view included only the breast.

Initial imaging studies, using a small camera outfitted with the collimator, were performed (*Task 13*) to determine some of the basic detection capabilities of the unit. The results were to be used in further optimization of the overall system configuration -- particularly, the distance between the camera and the breast being imaged.

Further optimization requires feedback from the system in terms of reconstructed images (*Task 11*), but these have not been generated yet.

*Task 13. Evaluate performance of modular camera.*

The performance of the small modular gamma camera was evaluated for the task of detecting small low-contrast signals in uniform and non-uniform random backgrounds. Detectability increased linearly with signal contrast and nonlinearly with signal diameter and decreased nonlinearly with increasing signal depth. For a signal contrast of 5.0, the camera was able to reliably detect (a) signals with diameters greater than 10 mm at a depth of 5 cm and (b) signals with 10 mm diameter at depths less than 6 cm. An average increase in contrast of about 38% was required to maintain a specified detectability when changing from uniform to non-uniform random backgrounds.

The use of straightforward signal detection theory was also shown, via a software model for the uniform random background case, to accurately predict camera performance for the task of detecting small low-contrast signals.

**Objective 3: Development of Software**

The tasks in this objective were to emulate the system point spread function (*Task 7*) and to develop an algorithm to generate three-dimensional reconstructions of the injected radiotracer activity (*Task 8*). The system point spread function provides a complete characterization of the detectors (cameras) for a given system configuration,

and the reconstruction algorithm, using both the point spread function and projection data, would allow for reconstructions of the spatial distribution of the radiotracer.

*Task 7. Emulate the system point spread function.*

The system point spread function has not been emulated. An effort was made (*Task 13*) to study the performance of a small camera prior to making final changes to the system geometry and measuring a system point spread function. The performance studies were completed very recently [1], and no results exist yet for a point spread function.

*Task 8. Develop an algorithm to generate three-dimensional reconstructions of the injected radiotracer activity.*

An algorithm has not been developed. As noted in the proposal, robust algorithms of the required type are already extensively used within this research group. An investigation of which algorithm might be best suited for this imaging system were supposed to begin once the principal investigator had both a system point spread function and projection data from each of the cameras. A system point spread function has not been measured, and so no work has been done on algorithm selection.

**Objective 4: Collection of Data and Reconstruction of Images**

The tasks in this objective were to collect and estimate projection data for the small cameras (*Task 9*) and the large camera (*Task 10*) and, if a point spread function had been measured (*Task 7*), to generate three-dimensional reconstructions of the radiotracer distribution (*Task 11*).

*Task 9. Collect and estimate projection data for small cameras.*

Projection data for the small camera was collected. The large breast phantom was imaged for both tumor-absent and tumor-present cases. For the tumor-present cases, the tumor-to-background ratio was 6:1.

*Task 10. Collect and estimate projection data for large camera.*

Projection data for the large camera was collected. As in *Task* 9, the object for the study was the large breast phantom. The small camera was used to collect four overlapping data sets and to generate a large composite image that would have been seen by the larger camera. No data was averaged or resampled in generating the composite image.

*Task 11. Generate three-dimensional reconstructions of the radiotracer distribution.*

Three-dimensional reconstructions of the radiotracer distribution have not been generated. A system point spread function has not been measured, and so no work has been done on reconstruction.

## Final Comments

The objectives completed in this grant generated useful knowledge that will help any future research on this or a similar project.

Objective 1 demonstrated that the objects to be visualized by this imaging system – lesions within a breast – will most likely contain an extremely small fraction of the injected radiotracer. So, a system designed for such a detection task must be very sensitive to small local uptakes of radiotracer within the breast while simultaneously ignoring the much larger amounts of out-of-field activity originating within the intrathoracic cavity. The phantoms constructed for testing purposes provide a good means of characterizing this sensitivity.

Objective 2 produced accurate laboratory characterizations and software models of the mean response and the performance of the small modular gamma cameras. The model for the mean response of the small cameras, while obviously providing needed information on the detector response in the emulation, allows for the design of cameras with different sizes and arrangements of scintillation crystals, light guides, and photomultiplier tubes. The model for the performance of the small cameras helps a system designer determine, for a given geometric configuration, what types of lesions might be detected.

## REFERENCES

[1] Sain JD, Barrett HH. "Performance evaluation of a modular gamma camera using detectability index." *J. Nucl. Med.* 2000; 41:176P.

## APPENDIX A – DOCUMENTATION FOR REVISED STATEMENT OF WORK

April 3, 2000

U.S. Army Medical Research and Materiel Command
Congressionally Directed Medical Research Program
MCMR-PLF (ATTN: Patricia C. Modrow, Ph.D.)
1077 Patchel Street
Fort Detrick, MD 21702-5024

RE: Grant No. DAMD17-97-1-7190 - "The Design and Emulation of a Multiple-Camera SPECT Breast Imager"

Dr. Modrow,

I just received the review of my Annual Report for Year 2 (submitted in June 1999). The cover letter for the review, written by Ms. Judy Pawlus on February 28, 2000, indicated that you, my Contracting Officer Representative, requested that I submit a revised Statement of Work.

The revised Statement of Work has been enclosed. Explanations for the revisions are detailed on a separate page.

Please let me know if any more information is required.

Sincerely,

John D. Sain, M.S.

Department of Radiology
The University of Arizona Health Sciences Center
1609 North Warren Avenue
Tucson, AZ 85724-5067

(520) 626-4267 (phone)
(520) 626-2892 (fax)

## STATEMENT OF WORK

### Objective 1: Construction of Breast Phantoms

**Task 1:** Months 1-3. Characterize the expected radiotracer activity (amounts and spatial distribution) within a human breast.

**Task 2:** Months 1-6. Design, procure materials for, and build breast phantoms.

### Objective 2: Design and Emulation of Imaging System

**Task 3:** Months 7-9. Characterize the response of the small gamma cameras.

**Task 4:** Months 7-9. Characterize the response of the large gamma camera.

**Task 5:** Months 10-36. Optimize the geometry of the system configuration.

**Task 13:** Months 25-34. Evaluate performance of modular camera.

### Objective 3: Development of Software

**Task 7:** Months 31-32. Emulate the system point spread function.

**Task 8:** Months 31-32. Develop an algorithm to generate three-dimensional reconstructions of the injected radiotracer activity.

### Objective 4: Collection of Data and Reconstruction of Images

**Task 9:** Months 17-20. Collect and estimate projection data for small cameras.

**Task 10:** Months 17-20. Collect and estimate projection data for large camera.

**Task 11:** Months 33-36. Generate three-dimensional reconstructions of the radiotracer distribution.

## STATEMENT OF WORK

### Yearly Accomplishments

**Year 1:** Construction of breast phantoms.
Characterization of modular cameras.
Initial optimization of system configuration.

**Year 2:** Development of software.
Initial collection/emulation of projection data.
Continued optimization of system configuration.

### Projected Yearly Accomplishments

**Year 3:** Continued collection/emulation of projection data.
Performance evaluation of modular camera.
Reconstruction of radiotracer activity in breast phantom.
Final optimization of system configuration.

**Explanation of revisions to Statement of Work**

**Task 5:** The time period for this task was changed from Months 10-12 to Months 10-36. The optimization of the geometry of the system configuration is an ongoing process. In an effort to continue improving the performance of the cameras, the optimization will continue as image data is collected and analyzed.

**Tasks 6 and 12:** These tasks have been eliminated. Due to (a) the reduced availability of the semiconductor array detectors within this research group and (b) the time constraints of the Principal Investigator's own graduate degree program, it is no longer reasonably feasible to accomplish this task.

**Task 13:** This task has been added to replace Tasks 6 and 12. An important aspect of the proposed imaging system is its ability to detect lesions within the breast. In particular, one would like to know the smallest lesion that the system can reliably detect and how the depth of the lesion within the tissue affects the system performance. The performance of the modular cameras for the task of detecting lesions as a function of diameter and depth will be measured. The results will aid in the continuing design of the imaging system.

**Tasks 7, 8, and 11:** The time period for these tasks was simply adjusted to reflect the loss of time in Year 2.

## APPENDIX B – POSTER PRESENTATION FOR TASK 13

This appendix contains a complete copy of the poster presentation made at *The Society of Nuclear Medicine 47th Annual Meeting* June 4-7, 2000, in St. Louis, MO. The title board of the presentation appeared as:

Performance Evaluation of a Modular Gamma Camera using Detectability Index

John D. Sain and Harrison H. Barrett

Dept. of Radiology and Optical Sciences Center
University of Arizona, Tucson, AZ

# INTRODUCTION

PURPOSE Signal detection theory is used to evaluate the performance of a modular gamma camera for the task of detecting small low-contrast signals in uniform and non-uniform random backgrounds. The experimental performance, achieved using real data, is compared to a theoretical computer model.

MOTIVATION We would like to estimate how well this camera may detect lesions in human breasts. The non-uniform random backgrounds in this study were designed to simulate planar projections of breast tissue observed in several clinical mammoscintigrams collected by the camera.

**SAMPLE MAMMOSCINTIGRAM**

(exposure time = 5 mins; counts in image = 40,000)

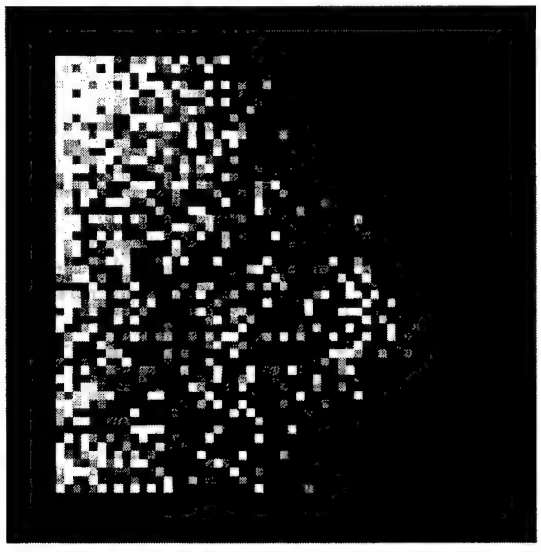

# SIGNAL DETECTION THEORY [1]

Signal detection is a form of binary hypothesis testing in which the hypothesis $H_1$ is that the signal is present and the alternative hypothesis $H_0$ is that it is absent. Using the available data, an observer decides, with some degree of error, whether $H_1$ or $H_0$ is true.

OBSERVER A channelized Hotelling observer was used in this study due to the limited number of sample image pairs. The channels, the $0^{th}$-$5^{th}$ orders of the Laguerre-Gauss family, were chosen not to mimic human performance but to estimate ideal performance.

DATA Each sample image consisted of a set of pixel values $\{g_m , m = 1,\ldots,M\}$ which were ordered as an Mx1 vector $\mathbf{g}$. There were 380 signal-present signal-absent image pairs.

TEMPLATE For a signal-known-exactly (SKE) study in which signal-absent and signal-present images are equally likely to occur and the signal has very low contrast, the channelized Hotelling template is

$$\mathbf{w_c} = \mathbf{K_c}^{-1} \mathbf{s_c}$$

where $\mathbf{K_c}$ is the channelized data covariance matrix and $\mathbf{s_c}$ is the channelized noise-free signal. $\mathbf{K_c}$ includes the effects of both measurement noise and randomness in the background.

TEST STATISTIC Using the channelized template $\mathbf{w_c}$ and sample images $\mathbf{g_c}$, an observer computes a test statistic $\lambda$ that is linear in $\mathbf{g_c}$, compares it to a threshold $\lambda_{th}$, and decides that $H_1$ is true if $\lambda > \lambda_{th}$.

$$\lambda = \mathbf{w_c}^t \mathbf{g_c}$$

FIGURES OF MERIT One means of specifying how well an observer can distinguish between $H_1$ and $H_0$ is to calculate a signal-to-noise ratio (SNR) defined by

$$SNR_\lambda^2 = \frac{[\langle \lambda \rangle_1 - \langle \lambda \rangle_0]^2}{[0.5\ \mathrm{var}_1(\lambda) + 0.5\ \mathrm{var}_0(\lambda)]}$$

where $\langle \lambda \rangle_k$ is the conditional expectation of $\lambda$ given that $H_k$ is true and $\mathrm{var}_k(\lambda)$ is the corresponding conditional variance. If $\lambda$ is normally distributed under both hypotheses, then the $SNR_\lambda$ is related to the area under the receiver operator characteristic (ROC) curve (AUC) by

$$AUC = 0.5 + 0.5\ \mathrm{erf}^{-1}(0.5\ SNR_\lambda),$$

and the detectability index, defined by

$$d' = 2\ \mathrm{erf}^{-1}(2\ AUC - 1),$$

is equal to the $SNR_\lambda$.

# HARDWARE IMAGES

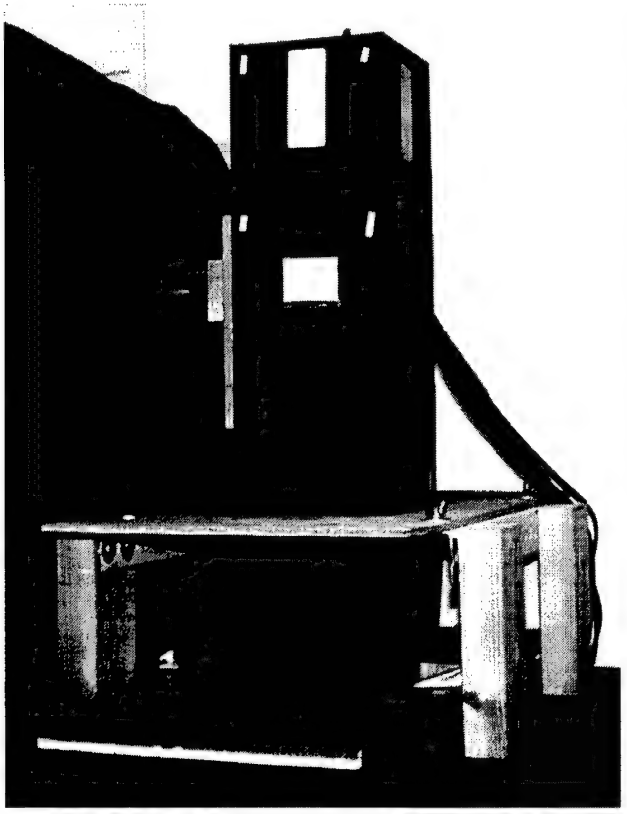

Experimental setup. The camera looks down into the water bath.

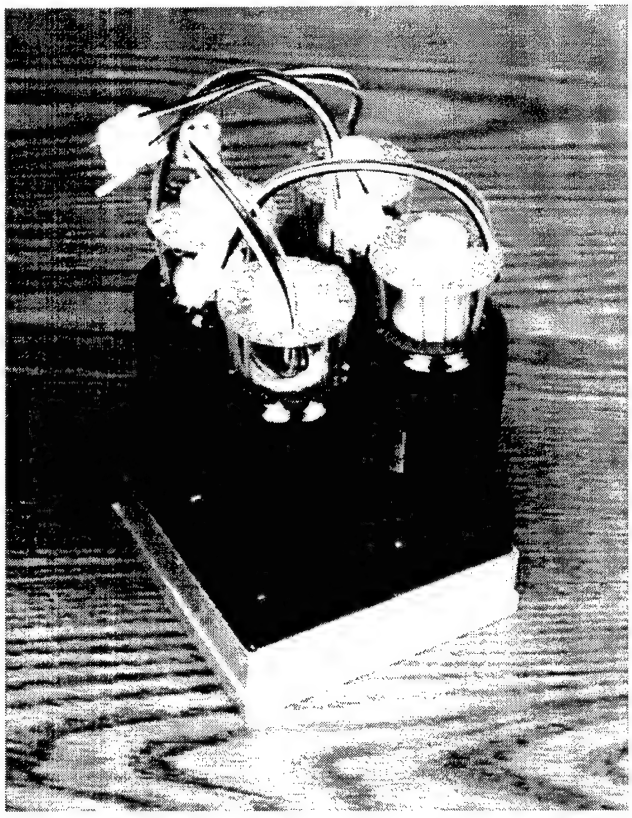

Camera components. A 10cm x 10cm NaI scintillation crystal, a 0.75" quartz light guide, and a 2x2 array of 2in x 2in PMT's.

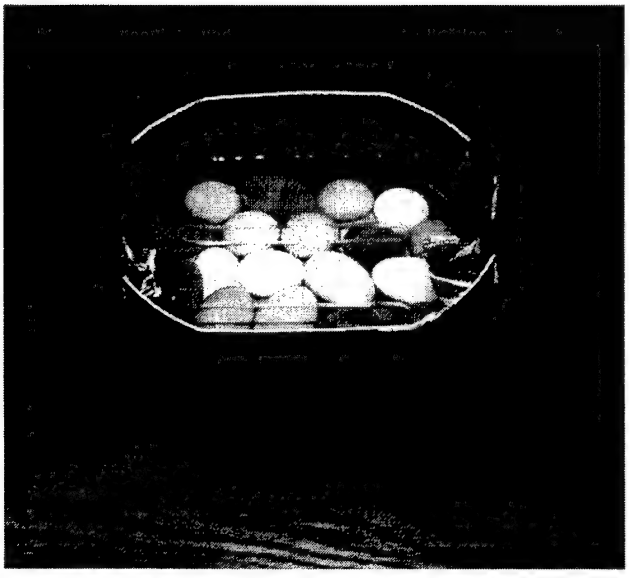

Water bath with eggs. 50 hollow plastic eggs filled with water and held 2.5 cm underwater with a 5-mm sheet of plexiglass.

Signal spheres. Several of the hollow plastic spheres used to simulate lesions.

# EXPERIMENTAL METHOD

## SIGNAL DATA

- Each data set ($20x10^6$ events) involved imaging a water-filled plastic sphere, injected with Tc-99m and set at a specific depth in the water bath.
- Six signal diameters (D = 4, 7, 10, 13, 16, 28 mm) at one depth (Z = 5 cm) and one signal diameter (D = 10 mm) at five depths (Z = 1, 3, 5, 7, 9 cm).

## BACKGROUND DATA

UNIFORM RANDOM

- One data set ($76x10^6$ events) with 20 mCi Tc-99m spread evenly throughout water.

NON-UNIFORM RANDOM

- 50 hollow plastic eggs (46 mm x 32 mm), filled with non-radioactive water, were placed in the water bath and held 2.5 cm underwater by a sheet of plexiglass.
- 760 data sets ($10^5$ events each) with 20 mCi Tc-99m spread evenly throughout water outside eggs.
- Prior to the collection of each data set, the eggs were stirred, resulting in a unique random pattern.

## IMAGE PAIRS

- 380 pairs of background images were generated by running background data through a maximum-likelihood position estimation look-up table.
- Signal data, for specified contrast (C), diameter (D), and depth (Z), was added to one image in each pair.

# SIGNAL

## SAMPLE IMAGE

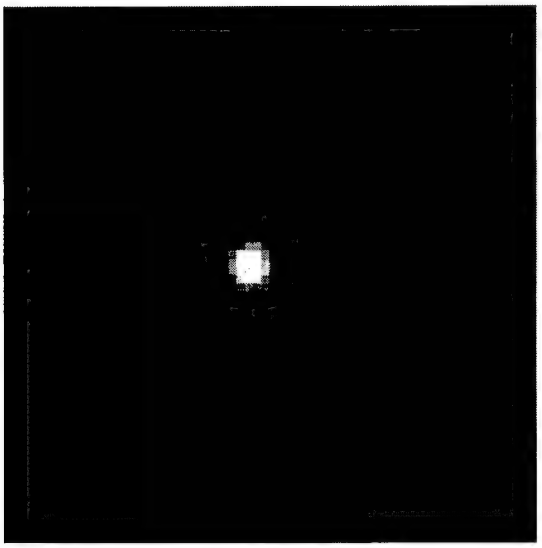

## CROSS-SECTION

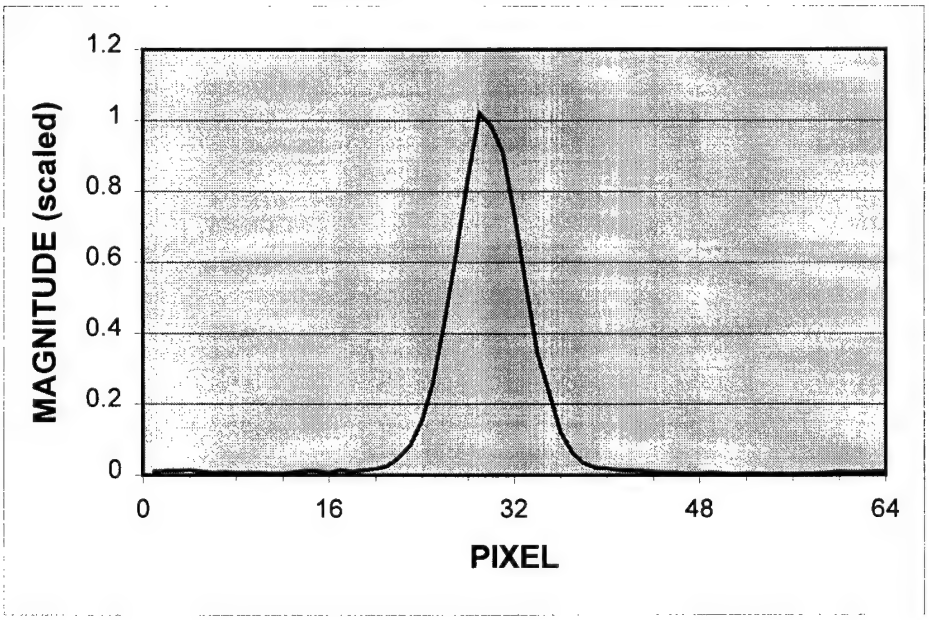

# IMAGE PAIRS

## UNIFORM RANDOM BACKGROUND

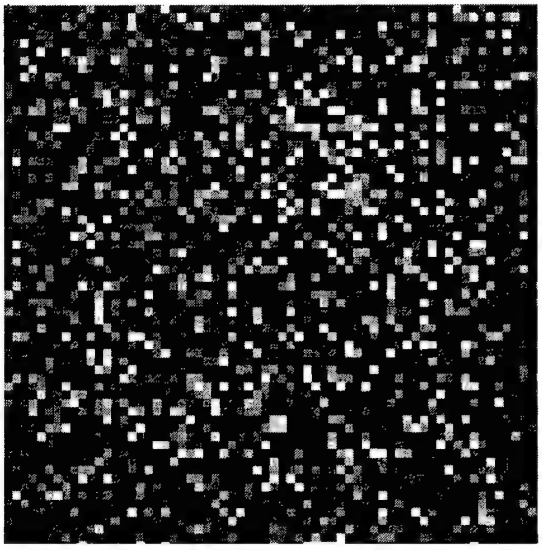

SIGNAL ABSENT

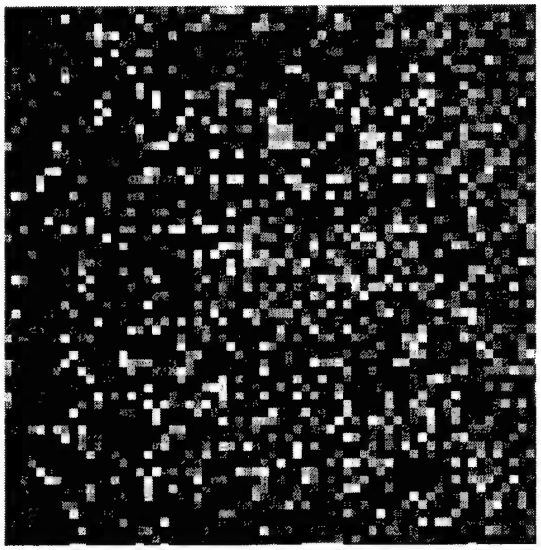

SIGNAL PRESENT

## NON-UNIFORM RANDOM BACKGROUND

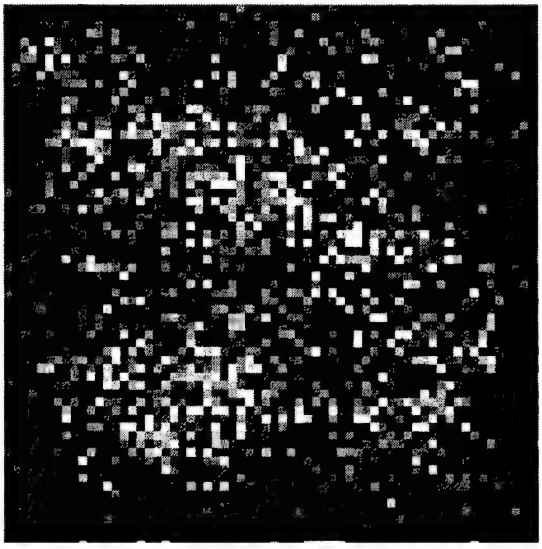

SIGNAL ABSENT

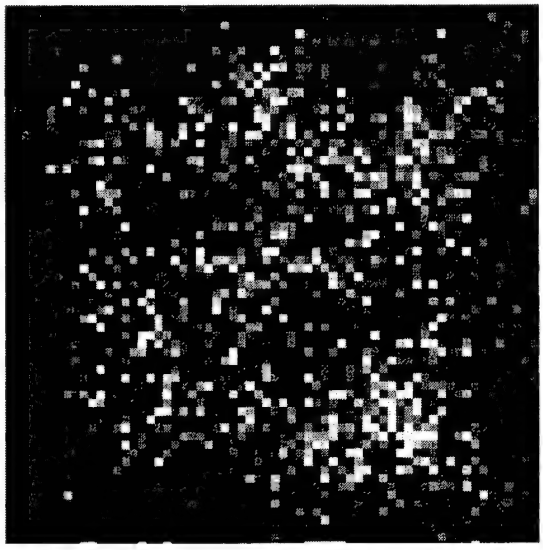

SIGNAL PRESENT

# IMAGING SCHEMATICS

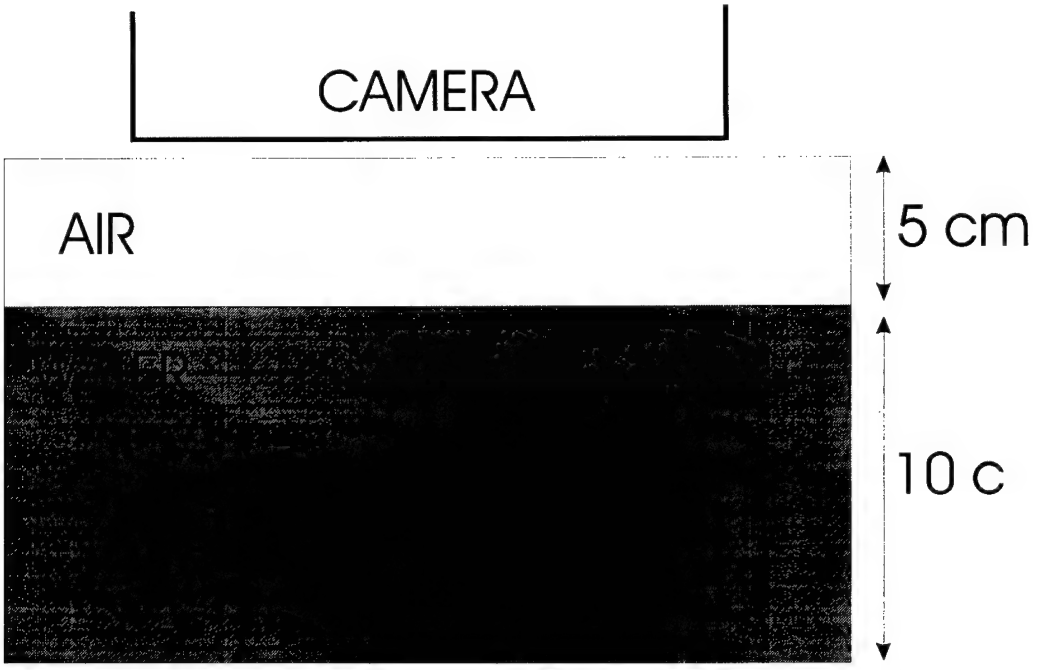


Experimental setup for collecting signal data.

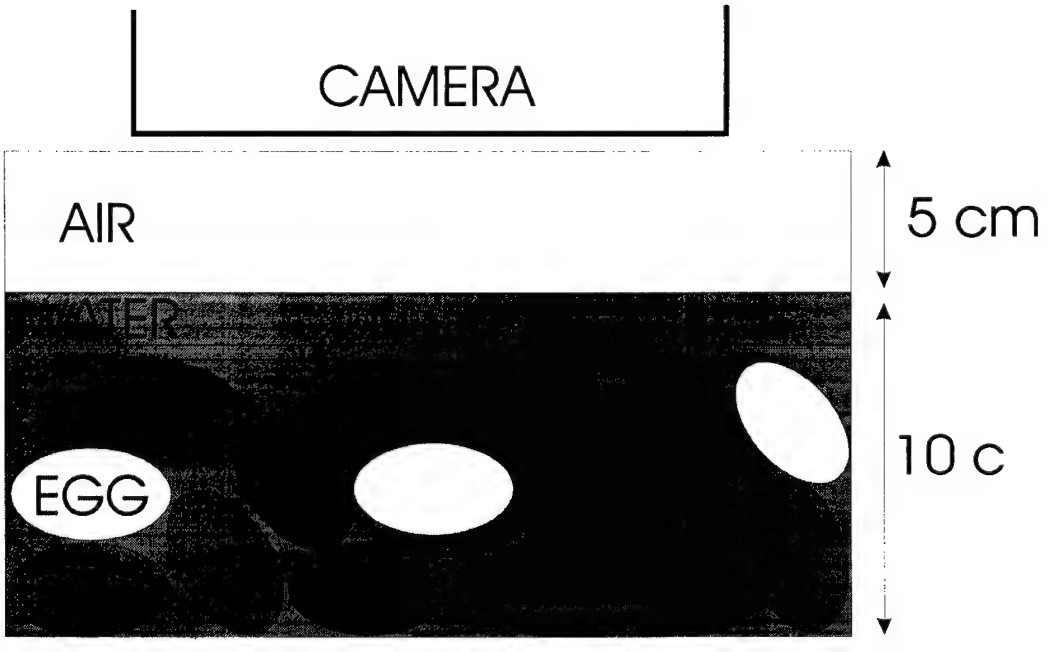


Experimental setup for collecting non-uniform random background data.

# EXPERIMENTAL RESULTS

- The C required to achieve a specified d' was greater for the non-uniform random background than for the uniform random background.
- d' increased linearly with C. [Fig. A]
- C increased nonlinearly with decreasing D for fixed d'. The rate of increase in C was significantly larger if D was less than the system's spatial resolution (9 mm).

  For the uniform case, the average slope of the log C vs. log D plots increased from –2.5 for larger diameter signals to –2.8 for smaller diameter signals. Similarly, for the non-uniform case, the average slope increased from –2.0 to –2.9. [Fig. B]
- For d' = 1.2 (or AUC = 0.8), the average increase in C for all D's, from the uniform to the non-uniform case, was 37%. The largest rise was 76% for D = 10 mm. [Fig. B]
- C increased nonlinearly with increasing Z for fixed d'. The rate of increase in C was larger for greater Z. [Fig. C]
- For d' = 1.2, the average increase in C for all Z's, from the uniform to the non-uniform case, was 38%. The percentage rose as Z increased –- from 19% for Z = 1 cm to 60% for Z = 9 cm. [Fig. C]

# FIG.A DETECTABILITY (d') vs. CONTRAST (C)

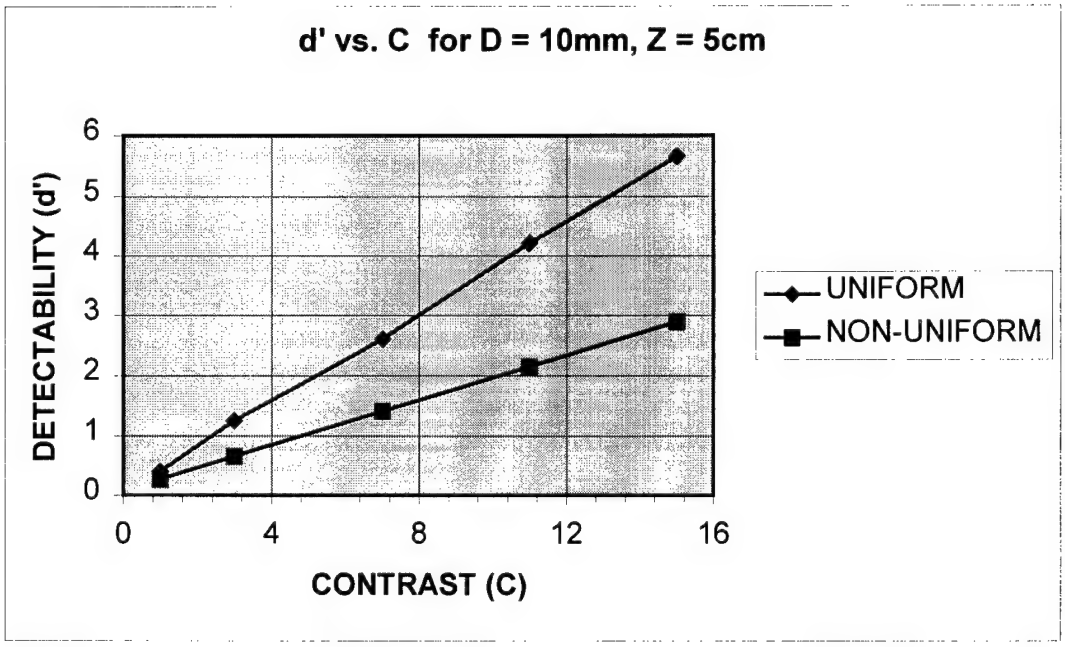


Contrast ≡ (Tumor-to-Background Ratio) -1

$$C = (A_S - A_B) / A_B$$

$$C = A_S / A_B - 1$$

$$C = TBR - 1$$

# FIG. B CONTRAST (C) vs. DIAMETER (D) [2,3,4]

## UNIFORM RANDOM BACKGROUND

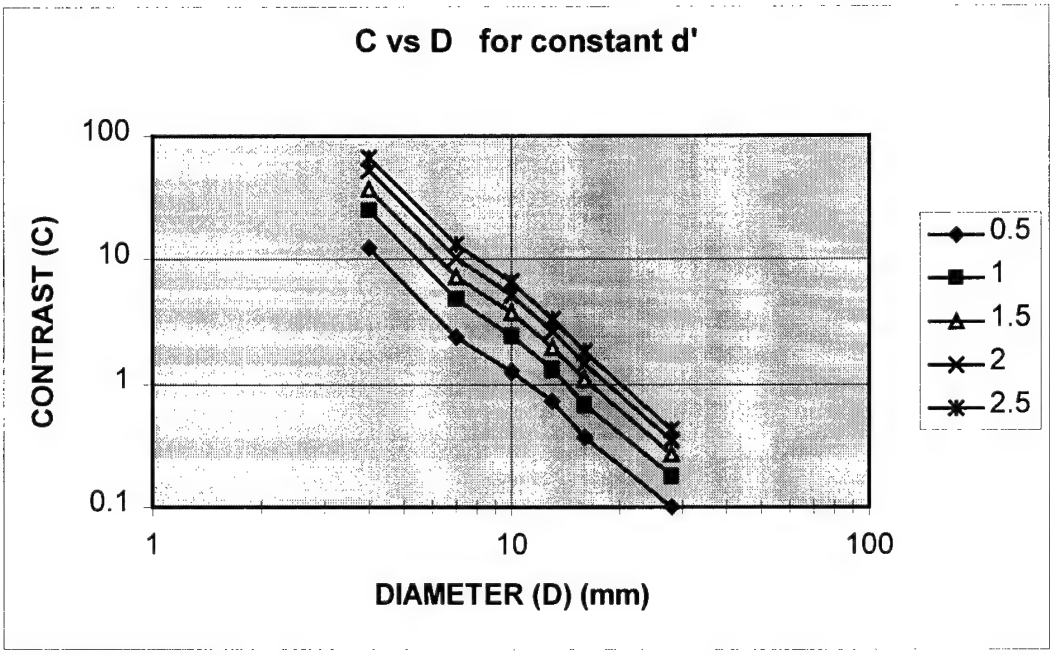


## NON-UNIFORM RANDOM BACKGROUND

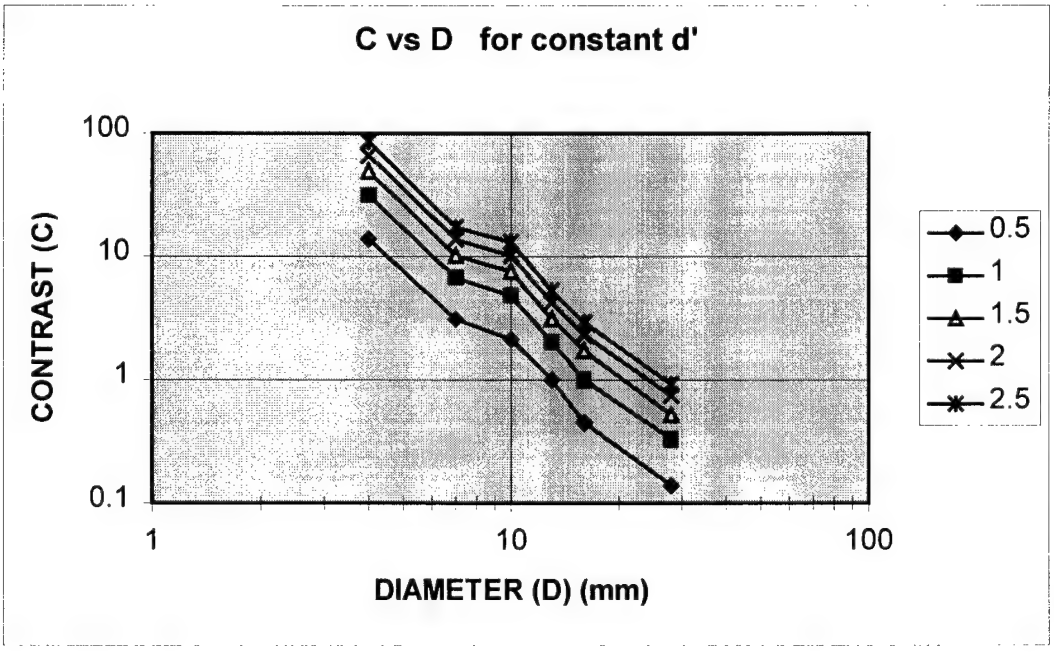

# FIG. C CONTRAST (C) vs. DEPTH (Z)

## UNIFORM RANDOM BACKGROUND

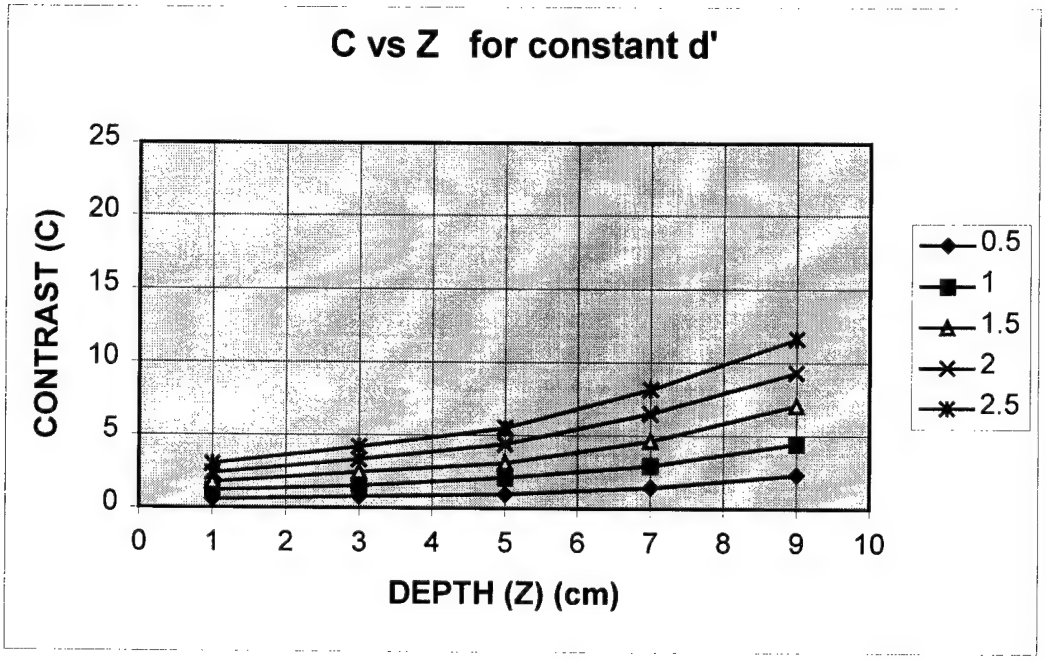


## NON-UNIFORM RANDOM BACKGROUND

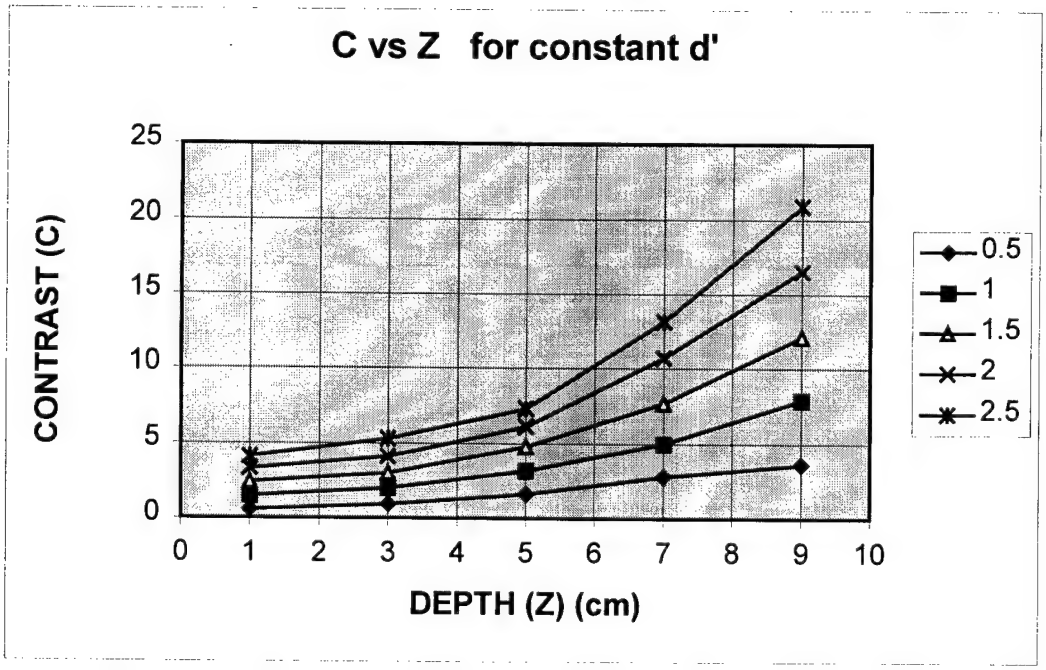

# THEORETICAL MODEL

## PURPOSE

- To simulate the laboratory experiment for the case of a uniform random background.

## DESCRIPTION

- The camera was modeled by a square (10 cm per side), pixellated (64 x 64) detector in the xy-plane.
- The water bath was represented by a cube (10 cm in each dimension) of uniform activity $A_B$.
- The signal was modeled by a sphere of diameter D and uniform activity $A_S$ and was located above the center of the detector at a depth of Z.
- The attenuation factor for both the signal and the background was assumed to be that of water.

## DIAGRAM

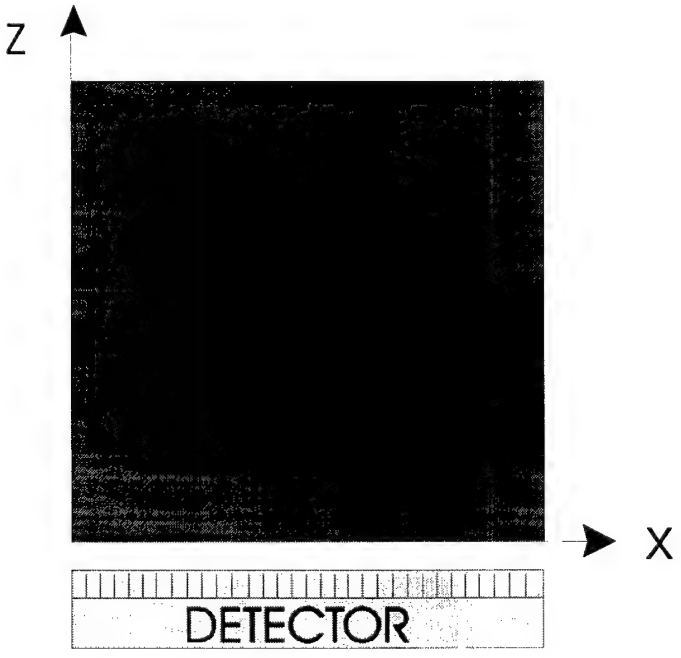

# METHOD

- The values of $A_B$, $A_S$, D, and Z were selected.
- The activity within the model was projected, along the z-axis, onto the detector.
- The geometric projection of the attenuated activity was convolved with a Gaussian kernel having a FWHM (9 mm) equal to the spatial resolution of the imaging system.
- The detectability was calculated from the 2-d projection data, $A_p(x,y)$, as

$$d' = \sqrt{\frac{\sum_{x,y} s^2(x,y)}{\overline{A}_p}} = \sqrt{\frac{\sum_{x,y} [A_p(x,y) - \overline{A}_p]^2}{\overline{A}_p}}$$

# RESULTS

- The theoretical model and experimental data agree.

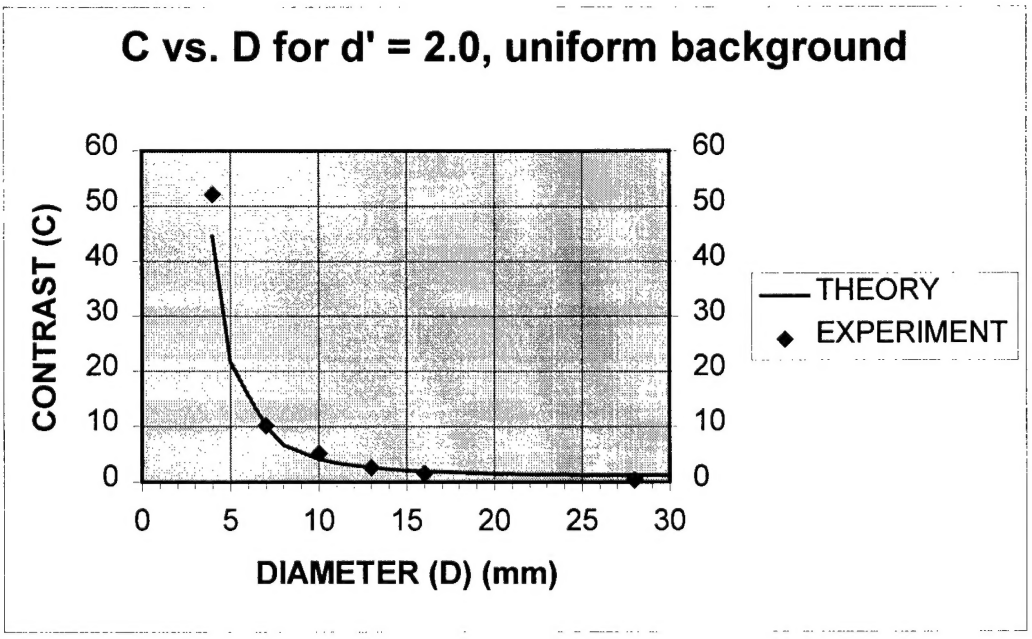

# CONCLUSIONS

- Straightforward signal detection theory predicts camera performance in the detection of small low-contrast signals. Experimental confirmation was shown in the case of uniform random backgrounds.
- Detectability *increases* linearly with signal contrast and nonlinearly with signal diameter.
- Detectability *decreases* nonlinearly with increasing signal depth.
- An average increase in contrast of about 38% was required to maintain a specified detectability when changing from uniform to non-uniform random backgrounds.
- While most breast lesions exhibit tumor-to-background ratios of about 1.5-3.0, certain types of breast carcinoma have been shown [5] to demonstrate average tumor-to-background ratios (TBR's) of nearly 6 (or average contrasts of nearly 5). For a contrast of 5, the camera evaluated in this study was able to reliably detect (a) signals with diameters greater than 10 mm at a depth of 5 cm and (b) signals with 10 mm diameter at depths less than 6 cm.

# REFERENCES

1. Barrett HH, Abbey CK, Gallas B, Eckstein M. "Stabilized estimates of Hotelling observer detection performance in patient-structured noise." *Proc. SPIE* 3340, 1998.
2. Wagner RF, Brown DG. "Overview of a unified SNR analysis of medical imaging systems." *IEEE Transactions on Medical Imaging*, 1982, Vol. MI-1, No.4, 210-214.
3. Wagner RF. "Low contrast sensitivity of radiologic, CT, nuclear medicine, and ultrasound medical imaging systems." *IEEE Transactions on Medical Imaging*, 1983, Vol. MI-2, No.3, 105-121.
4. Wagner RF and Brown DG. "Unified SNR analysis of medical imaging systems." *Phys. Med. Biol.*, 1985, Vol.30, No.6, 489-518.
5. Maublant J, de Latour M, Mestas D, et al.. "Technetium-99m Sestamibi uptake in breast tumor and associated lymph nodes." *J Nucl Med* 1996 (37) 922-925.

# ACKNOWLEDGEMENTS

U.S. Army Breast Cancer Research Program: DAMD17-97-1-7190
Center for Gamma Ray Imaging: PHS P41RR14304-01
SPECT Reconstruction Algorithms and Parallel Computing: RO1 CA52643

# ABSTRACT

**Objectives** The performance of a modular gamma camera for the task of detecting signals in random backgrounds was evaluated. The results were compared to a theoretical computer simulation.
**Methods** The camera uses a 10cm x 10cm NaI crystal, a 2x2 array of 2in x 2in PMT's, and a parallel-hole collimator (1.5mm bore width) and has 9mm spatial resolution (SR) at 5cm in water. It views a water bath (10cm deep) that fills its field of view. Uniform and non-uniform random background data was collected by imaging the bath containing 20 mCi Tc-99m. Non-uniformities were created by placing water-filled objects in the bath. Each signal data set was collected by imaging a water-filled plastic sphere, injected with Tc-99m and set at a specific depth (Z) in the bath. Data was collected for many signal diameters (D) (4, 7, 10, 13, 16, 28 mm) at one depth (5cm) and for one signal diameter (10mm) at several depths (1, 3, 5, 7, 9 cm). Sets of signal-present/signal-absent image pairs (380 pairs, 100k events/image) for known contrasts (C) were generated for use in ideal observer studies in which receiver operator characteristic (ROC) curves were plotted and the area under the ROC curve (AUC) and detectability index (d') were calculated. Contrast-detail (log C vs. log D) plots were created. The theoretical simulation, developed for uniform random backgrounds, provided data for comparison.
**Results** d' increased linearly with C and decreased nonlinearly with decreasing D or increasing Z. For C=3.1 and D=10mm, a d'=1.2 (or AUC=0.8) was obtained for Z=3cm. The C required to achieve a specific d' increased sharply for D<SR. Similar results were found for non-uniform backgrounds. The theoretical simulation verified the results for uniform random backgrounds.
**Conclusions** Straightforward signal detection theory predicts camera performance in the detection of small low-contrast signals.

## FINAL REPORT BIBLIOGRAPHY

Meeting abstracts

Sain JD and Barrett HH. "Performance evaluation of a modular gamma camera using detectability index." *J. Nucl. Med.* 2000, 41:176P.

Sain JD. "The design and emulation of a multiple-camera SPECT breast imager." *Proceedings of the 2000 Era of Hope Department of Defense Breast Cancer Research Program Meeting* Vol. 1, p.200.

Personnel receiving pay from the research effort

John D. Sain